

X-ray diffraction, magnetization and nuclear magnetic resonance study of $\text{Y}_2\text{Fe}_{17-x}\text{Ga}_x$

N X Shen[†], T K Daeubler^{†||}, J I Budnick[†], W A Hines[†], Y D Zhang[†],
D P Yang[‡], B G Shen[§] and Z H Cheng[§]

[†] Department of Physics and Institute of Materials Science, University of Connecticut, Storrs, CT 06269, USA

[‡] Department of Physics, College of the Holy Cross, Worcester, MA 01610, USA

[§] State Key Laboratory of Magnetism, Institute of Physics, Chinese Academy of Sciences, Beijing 100080, People's Republic of China

Received 17 March 1998

Abstract. A combined x-ray diffraction, magnetization and nuclear magnetic resonance (^{89}Y , ^{69}Ga and ^{71}Ga) study of the $\text{Y}_2\text{Fe}_{17-x}\text{Ga}_x$ system ($1 \leq x \leq 6$) is presented. It is found that the substitution of larger Ga atoms for Fe causes a transformation from the hexagonal to rhombohedral structure and an overall average lattice expansion of 2.7 \AA^3 per formula unit per Ga atom. Measurements on magnetically aligned powders yielded values for the anisotropy field and the average moment per Fe atom. Consistent with a change from planar to uniaxial anisotropy, the anisotropy field decreases with increasing Ga content and extrapolates to zero for $x \approx 7$. The average moment per Fe atom as well as the ^{89}Y hyperfine field also decrease with Ga content. Using a calculated value of $-0.40 \mu_B$ for the Y moment, values for the hyperfine coupling constants of $-120 \text{ kOe } \mu_B^{-1}$ and $-6.5 \text{ kOe } \mu_B^{-1}$ were obtained for the on-site and transferred contributions, respectively. The experimental results are discussed in terms of a model for the substitution of Ga for Fe in this system, and its relationship to the enhanced Curie temperature.

1. Introduction

It has been known for a long time that all of the binary rare-earth–(R–) iron R_2Fe_{17} intermetallic compounds have relatively low Curie temperature and easy plane anisotropy, thus inhibiting their use in permanent magnet applications. In recent years, however, much effort has been made to improve the hard magnetic properties of the R_2Fe_{17} compounds by interstitial and/or substitutional additions to the 2:17 structure. This effort was initiated by the discovery that introducing interstitial nitrogen or carbon atoms by means of gas–solid reaction [1–3] or melt spinning [4] resulted in an increase in the Curie temperature and saturation magnetization; and, in the case of $\text{Sm}_2\text{Fe}_{17}\text{N}_x$, changed the anisotropy from basal plane to uniaxial. (It is noteworthy that $\text{Sm}_2\text{Fe}_{17}\text{N}_x$ possesses better intrinsic hard magnetic properties than those of $\text{Nd}_2\text{Fe}_{14}\text{B}$ [5].) A volume expansion, which can be as much as 6% compared to the binary compounds, is observed in all of the interstitial compounds, along with the increase in the Curie temperature. In Fe-rich rare-earth–iron systems, the Curie temperature is mainly determined by the Fe–Fe exchange interaction, which is strongly dependent on the Fe–Fe interaction distance. Unfortunately, the interstitial compounds are

|| Also at: Department of Physics, University of Konstanz, D-78434 Konstanz, Germany.

thermodynamically unstable above 500 °C, and decompose into bcc α -iron and rare-earth nitrides. Therefore, the processing of these materials by conventional metallurgical means such as thermal sintering is hampered. A second breakthrough in this field occurred with the discovery that the replacement of some of the Fe atoms in R_2Fe_{17} by selected elements with a larger metallic radius resulted in stable compounds with an expanded lattice, and hence, increased Curie temperature [6–8]. Recently, investigations have been carried out on the substitutional $R_2Fe_{17-x}M_x$ systems, where M is a metalloid element such as Ga, Al or Si, or transition-metal element such as Ti, V, Co, Ni, Nb or Zr. All of these systems show an enhanced Curie temperature and, with the notable exceptions of Si and Co substitution, an increased volume per unit cell which can be as much as 9%. Despite the many studies, a complete understanding of the effect of the substituted element on the magnetic properties of the R and Fe sublattices is still lacking.

In this report, a combined x-ray diffraction, magnetization and nuclear magnetic resonance (NMR) study of the substitutional $Y_2Fe_{17-x}Ga_x$ system ($1 \leq x \leq 6$) is presented. In this system, the transition-metal Y takes the place of the rare-earth element; however, Y has a very small magnetic moment and makes no contribution to the magnetic anisotropy, thus enabling the behaviour of the Fe sublattice to be isolated. In previous work on the $Y_2Fe_{17-x}Ga_x$ system [9–13], it was determined that with the Ga substitution: (1) the volume per formula unit increases linearly up to $x = 8$ at a rate of 2.9 \AA^3 per Ga atom, (2) the Curie temperature increases and reaches a maximum ($\approx 200 \text{ K}$ above that for Y_2Fe_{17}) at $x \approx 3$ to 4 before decreasing and (3) the magnetic anisotropy changes from basal plane to uniaxial at $x \approx 6$ to 7. In addition to the crystal structure and bulk magnetic properties, this report focuses on the Fe magnetic moment behaviour as reflected in the hyperfine field (HF) measurements. A description of the Ga site selectivity is also presented.

2. Experimental apparatus and procedure

Ingots with nominal composition $Y_2Fe_{17-x}Ga_x$, $x = 1, 2, 3, 4, 5$ and 6, were prepared by arc melting using Y, Fe and Ga starting materials with a purity of 99.95%. Since yttrium has a relatively low boiling point and high vapour pressure, an additional amount of yttrium ($\leq 5\%$ by weight) was added to the starting materials in order to compensate for the loss during arc melting. The polycrystalline ingots were annealed in vacuum at approximately 900 °C for one week, and ground into powders with particle diameters in the range from 25 to 32 μm .

All x-ray diffraction powder patterns were obtained by employing Cu $K\alpha$ radiation and a Philips x-ray diffractometer which was equipped with a single-crystal monochromator. The diffraction intensity was recorded as a function of 2θ , the angle between the incident and the diffraction direction, using a home-made computer interface. The x-ray patterns were characteristic of those for the 2:17 compounds, having either the Th_2Ni_{17} -type hexagonal or Th_2Zn_{17} -type rhombohedral structure. The patterns for both structures can be indexed on hexagonal cells, and only differ in their stacking sequence along the c-direction, which is ABAB... for the hexagonal phase and ABCABC... for the rhombohedral phase. The a and c lattice parameters were obtained by performing a least squares fit to the diffraction peak 2θ -values.

In order to observe the magnetic anisotropy, samples consisting of fine powders were aligned at room temperature in a field of 16 kOe, and then fixed in epoxy resin. Magnetization (magnetic moment per unit mass) isotherms $M(H)$ were obtained at 10 K for magnetic fields up to 55 kOe using a Quantum Design SQUID magnetometer. The magnetization was measured in two directions, i.e., magnetic field both parallel and

perpendicular to the sample alignment direction. Before every measurement, the sample was completely demagnetized such that the magnetization curve obtained was the initial curve.

The zero-field spin-echo NMR spectra were collected at liquid helium temperatures using a phase coherent pulse spectrometer over the frequency range 12 to 50 MHz for the ⁸⁹Y isotope and a phase incoherent pulse spectrometer over the frequency range 35 to 180 MHz for the ⁶⁹Ga and ⁷¹Ga isotopes. Details of the methodology of NMR in magnetically ordered materials, including the experimental procedure and data acquisition, are available elsewhere [14].

3. Experimental results and analysis

Figure 1 shows the x-ray diffraction powder patterns for Y₂Fe_{17-x}Ga_x with Ga content $1 \leq x \leq 6$. Of the eight peaks labelled (*hkl*) in figure 1, six appear for both the Th₂Ni₁₇-type hexagonal and Th₂Zn₁₇-type rhombohedral structures (with the appropriate 2:3 ratio for *l*). The structure is uniquely identified by the characteristic peaks for each type, i.e., the (203) hexagonal peak at $2\theta = 41.0^\circ$ and (024) rhombohedral peak at $2\theta = 37.8^\circ$. (There is a trace of the (123) hexagonal peak (not labelled) at $2\theta = 46.5^\circ$. Also, there is a hexagonal (114) peak and a rhombohedral (215) peak; however, they both occur near $2\theta \simeq 49.1^\circ$ and are hard to distinguish.) The 2θ -values listed above are for the *parent* Y₂Fe₁₇ phase; the peaks shift to lower 2θ -values as the Ga content is increased. It can be seen in figure 1 for the $x = 1$ sample that the structure is completely hexagonal. With the substitution of

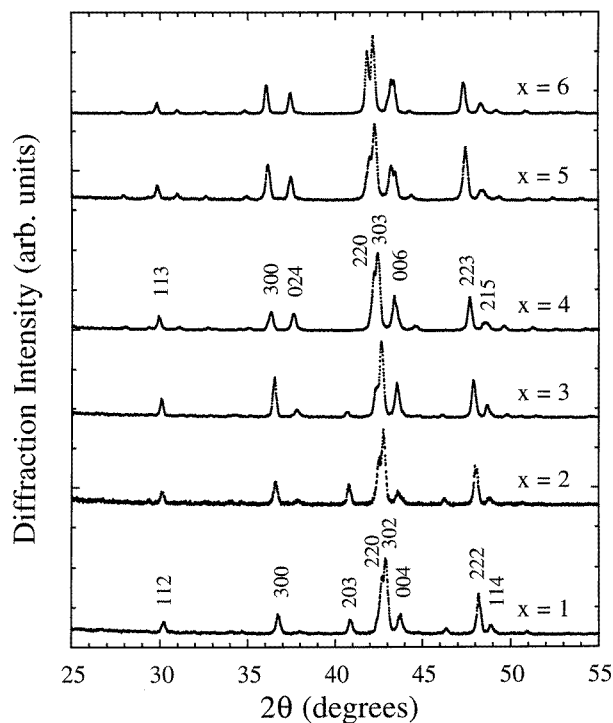


Figure 1. X-ray diffraction powder patterns for Y₂Fe_{17-x}Ga_x with $x = 1, 2, 3, 4, 5,$ and 6 . The structure transforms from hexagonal to rhombohedral as the Ga content increases. The transformation is complete when $x = 4$.

Ga for Fe in the lattice, the larger radius of the Ga atom makes the hexagonal structure unstable, and the rhombohedral structure starts to appear for $x = 2$. When the Ga content reaches $x = 4$, the transformation from hexagonal to rhombohedral is complete. In order to monitor the volume change upon substitution of Ga for Fe, the volume per formula unit, V_{fu} , was calculated using the a and c lattice parameters obtained by fitting 13 peaks in the x-ray diffraction patterns. Since the hexagonal structure has two formula units per unit cell whereas the rhombohedral has three, $V_{fu} = (a^2c \sin 60^\circ)/2$ for the former and $(a^2c \sin 60^\circ)/3$ for the latter. Also, since the two structures coexist for the $x = 2$ and $x = 3$ samples, the diffraction peaks from both structures were used to calculate the lattice parameters. It was found that the difference between the V_{fu} values for both structures lies within the experimental error.

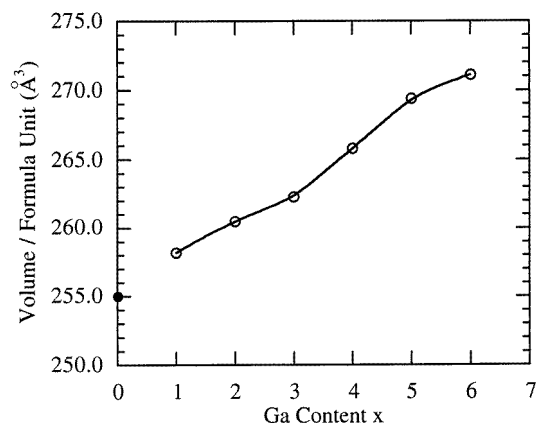


Figure 2. The volume per formula unit versus Ga content for $Y_2Fe_{17-x}Ga_x$ ($0 \leq x \leq 6$). The error bars are approximately the size of the symbols. The value for $x = 0$ was taken from [16].

Figure 2 shows the volume per formula unit versus Ga content for $Y_2Fe_{17-x}Ga_x$. Overall, the lattice expands as expected with increasing Ga content at an average rate of 2.7 \AA^3 per formula unit per Ga atom, consistent with Shen *et al* [9]. In addition, however, the curve shows a subtle change in slope at $x = 3$ and $x = 5$. A closer look at the lattice parameters used to calculate V_{fu} shows that the above behaviour is associated with c and not a . The lattice expansion along an a -axis is essentially linear with the Ga content whereas that along the c -axis shows the pronounced changes in slope at $x = 3$ and 5 referred to above. This is illustrated in figure 3 which shows the layer-layer distance L ($c/4$ for the hexagonal structure and $c/6$ for the rhombohedral structure) versus the Ga content for $Y_2Fe_{17-x}Ga_x$. As discussed below, the variation of L , and hence V_{fu} , has been attributed to the site selection preference as Ga replaces Fe in the lattice.

Figure 4 shows the magnetization M (in emu g^{-1}) versus the magnetic field H (in kOe) measured at 10 K for the six aligned samples of $Y_2Fe_{17-x}Ga_x$ ($1 \leq x \leq 6$). The \parallel notation indicates a direction of the magnetic field parallel to the alignment direction and \perp notation indicates a direction of the magnetic field perpendicular to the alignment direction. The area between the parallel curve and the perpendicular curve is a measure of the anisotropy energy. From this set of curves, it can be seen that the magnetic anisotropy originating from the Fe sublattice is reduced with the substitution of Ga. Values of the saturation magnetization M_s were obtained by fitting the various magnetization curves above 15 kOe to the form $M(H) = M_s - (A/H) - (B/H^2)$, and converted to Bohr magnetons per formula

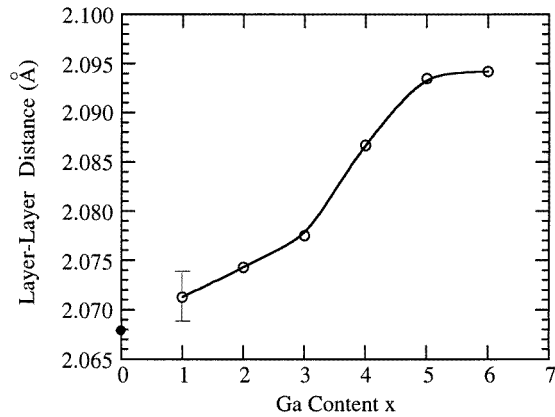


Figure 3. The layer-layer distance L versus Ga content for $Y_2Fe_{17-x}Ga_x$ ($0 \leq x \leq 6$), where L is $c/4$ for the hexagonal structure and $c/6$ for the rhombohedral structure. A typical error bar is indicated. The value for $x = 0$ was taken from [16]. There is a pronounced change in slope for $x = 3$ which is attributed to the Ga entry into the dumbbell $4f$ ($6c$) sites.

unit ($\mu_B \text{ fu}^{-1}$) using M_s ($\mu_B \text{ fu}^{-1}$) = M_s (emu g^{-1}) $\times W/5585$, where W is the formula unit weight (in g). In order to calculate an average value for the magnetic moment of a single Fe atom, $\langle \mu_{Fe} \rangle$, the moment value for yttrium is assumed to be $-0.4\mu_B$ and independent of the Ga content [15]. Also, it is assumed that gallium has no appreciable moment, and $\langle \mu_{Fe} \rangle$ can then be obtained from the measured saturation magnetization using

$$\langle \mu_{Fe} \rangle = \frac{M_2 (\mu_B \text{ fu}^{-1}) + 2 \times 0.4}{17 - x}. \quad (1)$$

Figure 5 shows $\langle \mu_{Fe} \rangle$ versus the Ga content for $Y_2Fe_{17-x}Ga_x$. It can be seen that the average Fe moment decreases with increasing Ga content; however, the behaviour of $\langle \mu_{Fe} \rangle$ is not linear and has a pronounced decline for $x > 3$. As discussed below, this behaviour is attributed to the site preference for the Ga atoms. Finally, values of the anisotropy field H_a (defined as $-2K_1/M_s$, where K_1 is the second order anisotropy constant) were extracted from the magnetization data in figure 4 using a simple model described by Li *et al* [12] H_a is calculated from the magnetic field value for which $(M_{\perp}/M_{\parallel}) = 0.935$. The magnetic field value is then corrected for demagnetization effects by using a demagnetization factor of $N \sim 1/10$ for the fixed fine powder samples [12]. Figure 6 shows H_a versus the Ga content for $Y_2Fe_{17-x}Ga_x$. It can be seen that H_a decreases with increasing Ga content and extrapolates to zero for $x \approx 7$, which is consistent with a change from planar to uniaxial anisotropy.

In an earlier work, a detailed ^{89}Y NMR study was carried out on hexagonal, rhombohedral and mixed phases of the Y_2Fe_{17} compound [16]. Hexagonal Y_2Fe_{17} has two Y sites designated 2b and 2d with HF values of -201.6 kOe (42.1 MHz) and -210.2 kOe (43.9 MHz), respectively. Rhombohedral Y_2Fe_{17} has one Y site designated 6c with a HF value of -204.0 kOe (42.6 MHz). (The negative sign indicates that the ^{89}Y the HF is opposite to the Fe sublattice magnetization.) Since the HF values for the three sites are approximately the same, the ^{89}Y NMR spectrum for a typical (hexagonal or mixed phase) sample of Y_2Fe_{17} will show a non-symmetrical broad peak centred near 42.6 MHz, with a shoulder on the high-frequency side. In order to understand the local atomic environment surrounding the Y sites and the interaction between a Y atom and its nearest neighbours, ^{89}Y NMR spectra were obtained at 4.2 K for the $Y_2Fe_{17-x}Ga_x$ samples with $1 \leq x \leq 6$ (see

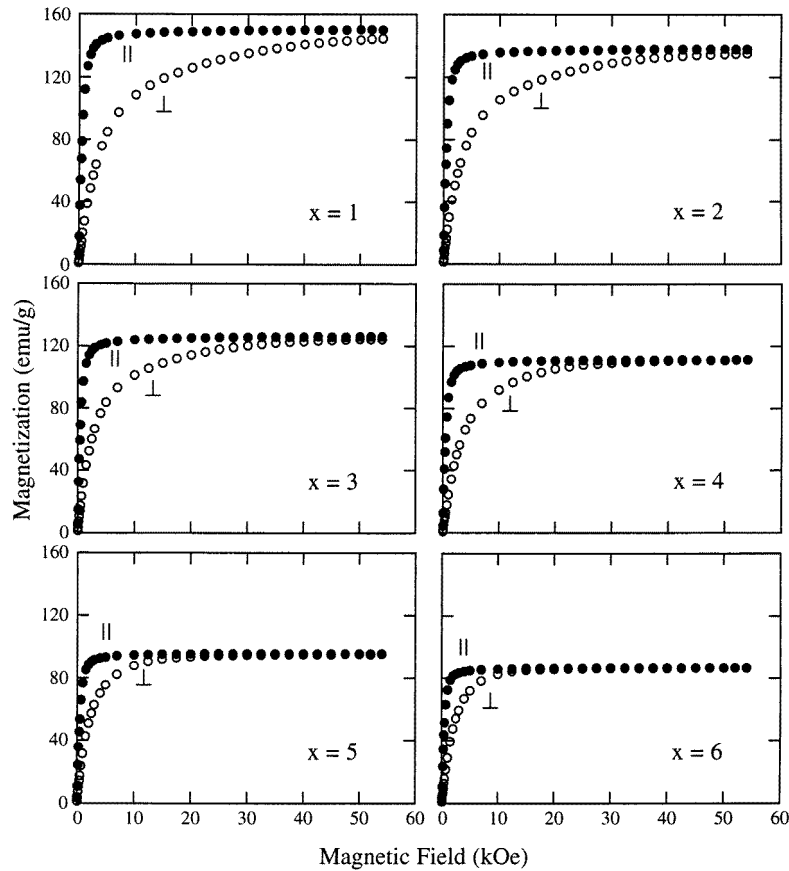


Figure 4. Magnetization M (in emu g^{-1}) versus magnetic field H (in kOe) measured at 10 K for aligned samples of $\text{Y}_2\text{Fe}_{17-x}\text{Ga}_x$ with $x = 1, 2, 3, 4, 5,$ and 6 ; \parallel indicates applied field parallel to alignment direction and \perp indicates applied field perpendicular to alignment direction.

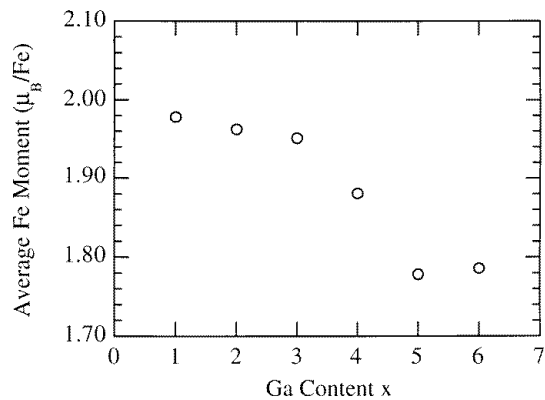


Figure 5. The average magnetic moment value for a single Fe atom (μ_{Fe}) (in μ_B) versus Ga content for $\text{Y}_2\text{Fe}_{17-x}\text{Ga}_x$ ($1 \leq x \leq 6$). There is a pronounced decrease in moment value when $x > 3$.

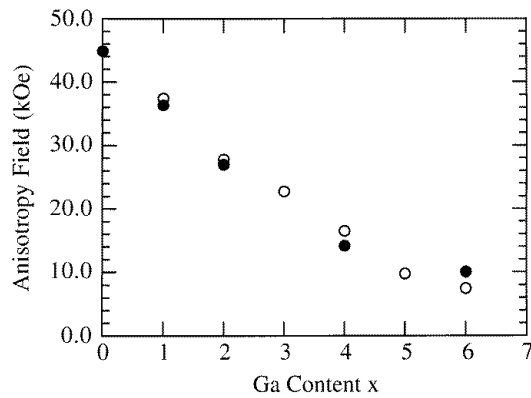


Figure 6. The anisotropy field H_a (in kOe) versus Ga content for $Y_2Fe_{17-x}Ga_x$ ($1 \leq x \leq 6$): open circles—this work; closed circles—[12].

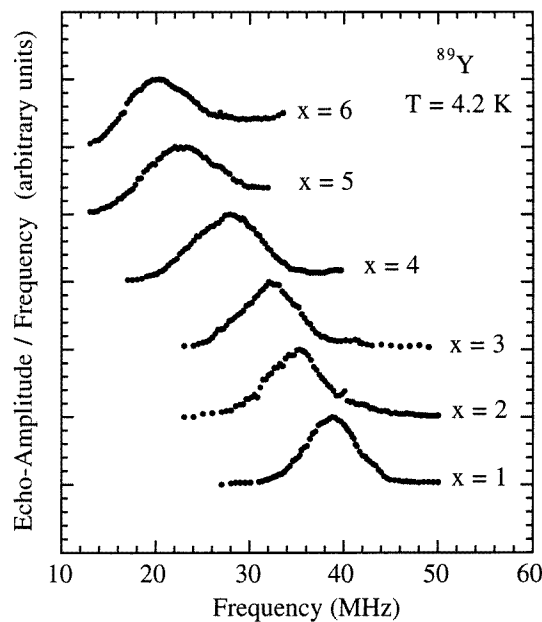


Figure 7. ^{89}Y zero-field spin-echo NMR spectra obtained at 4.2 K for $Y_2Fe_{17-x}Ga_x$ with $x = 1, 2, 3, 4, 5$ and 6 .

figure 7). From figure 7, it can be seen that the average hyperfine field of ^{89}Y , as measured by the peak frequency, decreases as the Ga content increases. This result is expected since Ga has no magnetic moment and the replacement of Fe by Ga dilutes the local magnetization. In addition, the average Fe moment also decreases (see figure 5). It will be shown later that the behaviour of the HF for ^{89}Y parallels that of $\langle \mu_{Fe} \rangle$ illustrated in figure 5. The ^{89}Y peak broadens with Ga substitution and the high-frequency shoulder is obscured. However, no ^{89}Y satellite peaks are observed for any of the $Y_2Fe_{17-x}Ga_x$ samples. This is in contrast to the case for $Y_2Fe_{17}N_x$, in which the strong interaction between nitrogen interstitial atoms and the lattice splits the ^{89}Y NMR spectrum into different peaks, corresponding to the Y

atoms with different numbers of nitrogen as the nearest neighbours [17]. A quantitative analysis of the ^{89}Y HF behaviour and coupling constants is now presented.

Since the gallium atoms have no moment, the HF for ^{89}Y can be assumed to consist of three contributions

$$\text{HF}(^{89}\text{Y}) = H_{cp} + H_s + H_{sp} \quad (2)$$

where H_{cp} is the core polarization due to the exchange interaction between the on-site Y moment and the inner s electrons, H_s is the spin polarization of the conduction s electrons due to the on-site Y moment and H_{sp} is the conduction electron spin polarization that is transferred from the nearest neighbour Fe moments. The first two terms, $H_{cp} + H_s$, are directly proportion to the Y moment μ_Y (which is taken to be $-0.40 \mu_B$) [15], and the third term can be written as

$$H_{sp} = \sum_i \alpha_i n_i \mu_{Fe}(i) \quad (3)$$

where $\mu_{Fe}(i)$ is the magnetic moment of the neighbouring Fe atoms at the i -type site, n_i is the number of i -site Fe atoms surrounding the Y atom and α_i is the hyperfine coupling constant. (As described later, there are four distinct Fe sites in this system.) In order to obtain values for the on-site and transferred hyperfine coupling constants, we can approximate the summation by taking $H_{sp} \approx \alpha n \langle \mu_{Fe} \rangle$, where α is an average value for the transferred hyperfine coupling constant, $\langle \mu_{Fe} \rangle$ is the average Fe moment from figure 5, and $n = 19(17-x)/17$ is the number of nearest neighbour Fe atoms. (For $\text{Y}_2\text{Fe}_{17-x}\text{Ga}_x$, the Y 2b and 2d sites in the hexagonal structure have 18 and 20 Fe/Ga atoms as nearest neighbours, respectively, while the Y 6c sites in the rhombohedral structure have 19 Fe/Ga atoms as nearest neighbours.) The $(-)\text{HF}(^{89}\text{Y})$ values are then calculated from the resonance peak frequencies for the six spectra shown in figure 7 using $\gamma(^{89}\text{Y}) = 0.20859 \text{ MHz kOe}^{-1}$. Figure 8 shows $\text{HF}(^{89}\text{Y})$ versus $n \langle \mu_{Fe} \rangle$ for $\text{Y}_2\text{Fe}_{17-x}\text{Ga}_x$ ($1 \leq x \leq 6$), where the Ga content is an internal parameter. From the slope, a value of $\alpha = (-)6.5 \text{ kOe } \mu_B^{-1}$ is obtained for the average transferred hyperfine coupling constant. From the intercept, $H_{cp} + H_s = (+)47 \text{ kOe}$, and by taking $\mu_Y = -0.40 \mu_B$, the on-site hyperfine coupling constant $\beta = (-)120 \text{ kOe } \mu_B^{-1}$ is obtained. From the available data, it is impossible to separate the H_{cp} and H_s contributions. However, it is usually the case that the core polarization term is dominant and negative.

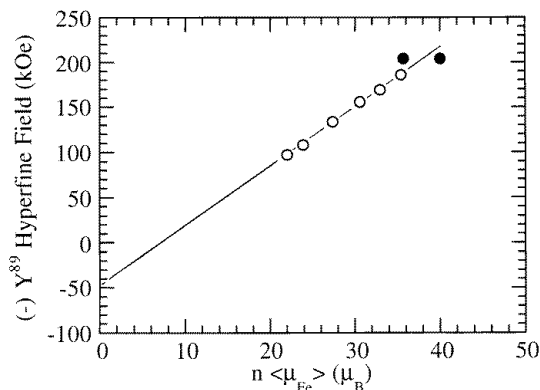


Figure 8. The ^{89}Y hyperfine field (in kOe) versus the total nearest neighbour magnetic moment $n \langle \mu_{Fe} \rangle$ (in μ_B) for $\text{Y}_2\text{Fe}_{17-x}\text{Ga}_x$ ($1 \leq x \leq 6$)—open circles. The values for $x = 0$ were taken from [12] and [16]—closed circles.

In order to gain insight into the site preference of Ga in $Y_2Fe_{17-x}Ga_x$, an NMR investigation of the ^{69}Ga and ^{71}Ga isotopes was carried out. As NMR probes, both ^{69}Ga and ^{71}Ga nuclei have the advantage of high natural abundance, which is 60.4% and 39.6%, respectively. As an impurity in bcc α -Fe, Ga has a transferred hyperfine field of approximately 100 kOe which corresponds to ^{69}Ga and ^{71}Ga resonances near 100 MHz and 125 MHz, respectively [18]. As revealed by neutron diffraction [19] and Mössbauer [20] measurements, Y_2Fe_{17} has four distinct iron sites, 4f (6c), 6g (9d), 12j (18f) and 12k (18h) for the hexagonal (rhombohedral) structure. If Ga substitutes for Fe at any of these sites, the hyperfine fields for the Ga isotopes, which are also determined by the nearest neighbour environment, will depend on which Fe atoms have been replaced by Ga. Therefore, if the Ga substitution has any site preference, it will be reflected in the NMR spectra for the Ga isotopes. Figure 9 shows the ^{69}Ga and ^{71}Ga NMR spectra for $Y_2Fe_{17-x}Ga_x$ ($1 \leq x \leq 6$). The spectrum for $x = 1$ clearly shows two well separated peaks, located at 125 MHz and 155 MHz. Considering the relative intensity ratio of the two peaks, and the different values of the gyromagnetic ratio ($\gamma = 1.022 \text{ MHz kOe}^{-1}$ and $1.298 \text{ MHz kOe}^{-1}$ for ^{69}Ga and ^{71}Ga , respectively), the peaks at 125 MHz and 155 MHz are attributed to ^{69}Ga and ^{71}Ga , respectively. The shape of both peaks appears to be Gaussian, therefore, it is reasonable to conclude that the spectrum arises from Ga at a single site. Since Ga has negligible magnetic moment and the HF for ^{69}Ga and ^{71}Ga is only that transferred from the nearest neighbour Fe atoms, the resonance peak(s) shift to lower frequency as the Ga content is increased. The peaks corresponding to the two isotopes can still be barely resolved for $x = 2, 3$ and 4; however, for $x = 5$ and 6, only one broad peak is observed. This is consistent with Ga entering more than one type of site for higher Ga content.

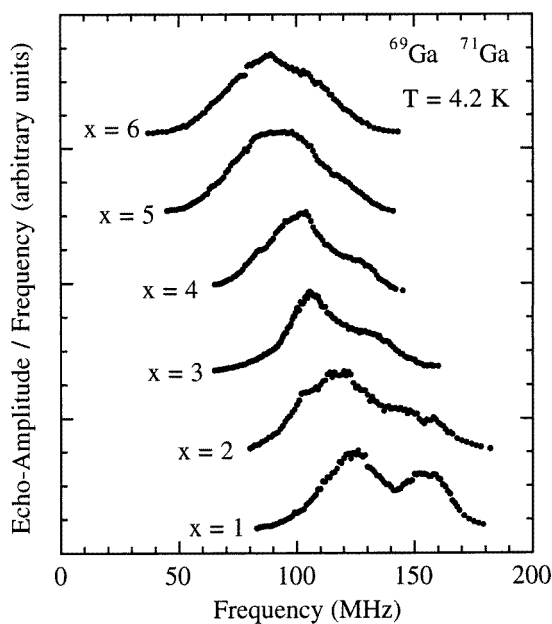


Figure 9. ^{69}Ga and ^{71}Ga zero-field spin-echo NMR spectra obtained at 4.2 K for $Y_2Fe_{17-x}Ga_x$ with $x = 1, 2, 3, 4, 5$ and 6.

4. Discussion and conclusions

The combined x-ray diffraction, magnetization and nuclear magnetic resonance results presented above will be discussed in the light of a proposed model for the substitution of Ga for Fe in $Y_2Fe_{17-x}Ga_x$. The hexagonal Y_2Fe_{17} structure has two Y sites, 2b and 2d. Yttrium 2b has six Fe(6g), six Fe(12j), six Fe(12k) and no ‘dumbbell’ Fe(4f) as nearest neighbours, while Y 2d has three Fe(6g), six Fe(12j), nine Fe(12k) and two dumbbell Fe(4f) as nearest neighbours. On the other hand, the rhombohedral Y_2Fe_{17} structure has a single Y site, 6c, which has three Fe(9d), six Fe(18f), nine Fe(18h) and one dumbbell Fe(6c) as nearest neighbours. As discussed in an earlier work, disordering and deviation from the 2:17 stoichiometry in the hexagonal phase will result in an incomplete occupancy of the 2b sites [16].

In terms of the crystal structure, the substitution of Ga for Fe in $Y_2Fe_{17-x}Ga_x$ causes a transformation from the hexagonal phase which exists for $x = 1$ to the rhombohedral phase for $x \geq 4$, with $x = 2$ and 3 being mixed phase (see figure 1). This is consistent with earlier observations of the hexagonal Th_2Ni_{17} -type structure being made unstable by Ga substitution [13,21]. As expected, the replacement of the Fe atoms by the larger Ga atoms results in an expansion of the lattice as reflected by the general increase in the volume per formula unit shown in figure 2. In particular, it was observed that the lattice parameter a increases in a nearly linear fashion with increasing Ga content; however, the lattice parameter c (or layer–layer distance) shows an abrupt change in slope for $x = 3$ (see figure 3). This can be attributed to the onset of Ga atoms entering the dumbbell sites (hexagonal 4f or rhombohedral 6c) when the Ga content reaches $x = 3$. As the dumbbell sites are squeezed between the rare-earth planes in the 2:17 structure, the substitution of the larger Ga atoms will expand the c lattice parameter significantly.

Further evidence for the site substitution pattern described above comes from both the magnetization and NMR results. Two independent, and yet consistent, measurements of the average magnetic moment per single Fe atom were obtained from the saturation magnetization (figure 5) and the ^{89}Y transferred HF. The decrease in the saturation magnetization is not just due to dilution by replacing Fe with Ga. As a function of the Ga content x , the value of $\langle\mu_{Fe}\rangle$ shows an abrupt change in slope at $x = 3$, declining more rapidly. It was observed that the ^{89}Y HF behaviour parallels that for $\langle\mu_{Fe}\rangle$, with values of $-120 \text{ kOe } \mu_B^{-1}$ and $-6.5 \text{ kOe } \mu_B^{-1}$ being obtained for the on-site and transferred hyperfine coupling constants, respectively. From previous neutron diffraction [19] and Mössbauer effect [20] experiments on Y_2Fe_{17} , it was determined that the Fe atoms at the dumbbell sites have the largest magnetic moment; the Fe moment values for the four inequivalent hexagonal (rhombohedral) sites follow the order $\mu_{4f}(\mu_{6c}) > \mu_{6g}(\mu_{9d}) > \mu_{12j}(\mu_{18f}) > \mu_{12k}(\mu_{18h})$. Therefore, the replacement of Fe by Ga at the dumbbell sites when $x \geq 3$ will greatly reduce the total moment, and hence, $\langle\mu_{Fe}\rangle$ as well as HF(^{89}Y).

Based on the spectra of the ^{69}Ga and ^{71}Ga isotopes for $x = 1$, it appears that Ga predominately enters only one type of Fe site. For $x \geq 5$, multiple site occupancy seems reasonable. However, to determine which types of Fe site the Ga atoms enter is not straightforward. Considering size limitations, the Fe(6g) sites in the hexagonal structure are probably too small (Fe site with the smallest Wigner–Seitz cell volume) to accommodate the Ga atoms. Therefore, the remaining sites available for the initial occupation by Ga atoms will be the Fe(12j) and Fe(12k) sites. Although both types of site are nearest neighbours to the Y sites, the Fe(12j) sites are in the same plane as

the Y sites. Compared to iron, the radius for yttrium is much larger and, therefore, the distortion in the rare-earth plane would be more severe than in the iron–iron plane. As a result, it might be expected that the initial entry of Ga will occur at the Fe(12k) sites as the entry of Ga into the Fe(12j) sites would create a much larger strain. Furthermore, based on the neutron diffraction [19] and Mössbauer effect [20] results cited above, the Fe atoms at the 12k sites have the smallest moment. The filling of the 12k sites will produce the smallest reduction in the average moment. This is consistent with a Mössbauer study by Morariu *et al* [22] on $Y_2Fe_{17-x}M_x$ compounds, with $M = Al, Ga$ and Si , and $x = 1$ and 2 . Their results indicate an initial entry by these nonmagnetic M atoms into the hexagonal Fe(12k) sites. It is concluded that for the $Y_2Fe_{17-x}Ga_x$ system studied in this work, the Ga atoms initially enter only the hexagonal Fe(12k) sites. For $x = 3$, there is an onset of Ga atoms entering the dumbbell (hexagonal 4f or rhombohedral 6c) sites.

A detailed knowledge of how Si, Al and Ga substitute for Fe in the R_2Fe_{17} compounds is crucial for understanding the microscopic origin of the large T_c enhancement which occurs in these materials. In the case of insertion of gas phase elements into the interstitial sites, the explanation seems straightforward. The large increase in T_c is attributed to the expansion of the lattice ($\leq 6\%$) that comes with the accommodation of the interstitial atoms, along with the well known dependence of the Fe–Fe exchange interactions on interatomic distance. Generally speaking, substitutional systems also exhibit lattice expansion ($\leq 9\%$) along with the T_c enhancement; however, there are notable exceptions. For example, the substitution of Si for Fe in $Y_2Fe_{17}Si_x$ increases T_c even though the lattice contracts [23]. An alternative explanation for the enhancement of T_c in the substitutional systems is based on the preferential substitution of Si, Al and Ga for Fe at the dumbbell sites which leads to a disappearance of Fe–Fe antiferromagnetic interactions at these sites [24]. For the $Y_2Fe_{17-x}Ga_x$ system reported here, T_c increases with the Ga content and reaches a maximum at $x \approx 3$ to 4 before decreasing [11, 12]. With the substitution pattern developed above, Ga entry into the dumbbell sites does not occur until $x = 3$, which is not low enough to account for the T_c enhancement. Consequently, it appears that lattice expansion is responsible for the T_c enhancement in $Y_2Fe_{17-x}Ga_x$. Concerning the issues of preferential site selection and T_c enhancement, two previous reports are particularly relevant to the results presented here. For the Y_2Fe_{17} parent system and Si substitution, Ge *et al* [23] have carried out a ^{89}Y NMR study on hexagonal $Y_2Fe_{17-x}Si_x$ and report that the Si atoms do preferentially enter the dumbbell 4f sites for $x \leq 1.0$. This conclusion is based on the separation of the 2b and 2d ^{89}Y peaks, and the fact that Y(2b) has two dumbbell Fe atoms as nearest neighbours while Y(2d) has none. They attribute the increase in T_c to the preferential substitution. The NMR results reported by Ge *et al* [23] however, appear to be inconsistent with the Mössbauer results of Morariu *et al* [22] cited above. On the other hand, for Ga substitution into the Nb_2Fe_{17} and Tb_2Fe_{17} parent systems, Hu *et al* [25] have carried out both Mössbauer effect and neutron diffraction studies on rhombohedral $Nb_2Fe_{17-x}Ga_x$ and $Tb_2Fe_{17-x}Ga_x$, and find that Ga completely avoids the 9d sites, occupies the 6c dumbbell sites only for $x \geq 5$, and strongly prefers the 18f sites for large x . Consequently, they conclude that the initial T_c enhancement in these systems is not a result of the replacement of Fe(6c) atoms by Ga. From the work to date on the substitutional systems, a picture of the T_c enhancement is emerging; however, a complete understanding is still lacking.

Finally, the values of $\langle \mu_{Fe} \rangle$ in figure 5 were calculated from the saturation magnetization using a correction of $-0.40 \mu_B$ for the Y moment which was obtained from band structure calculations for Y_2Fe_{17} [15]. This is also consistent with experimental work on other Y–Fe

compounds [26, 27]. It should be noted that using a smaller value for the Y moment will not change the value obtained for the transferred hyperfine coupling constant ($-6.5 \text{ kOe } \mu_B^{-1}$) which was obtained from the slope in figure 8. On the other hand, the value obtained for the on-site hyperfine coupling constant will be increased. Previous theoretical work concerning the core polarization contribution in 4d ions indicates that hyperfine coupling constants exist which are two or three times larger than the value of $-120 \text{ kOe } \mu_B^{-1}$ obtained here [28]. If this is the case, it would suggest that the magnitude of calculated Y moment value is too large.

Acknowledgments

The authors wish to thank Professors A J Freeman and W B Yelon for very helpful discussions. This work was supported by NSF grant DMR-9705136.

References

- [1] Coey J M D and Sun H 1990 *J. Magn. Magn. Mater.* **87** L251
- [2] Liao L X, Chen X, Altounian Z and Ryan D H 1992 *Appl. Phys. Lett.* **60** 129
- [3] Zhong X P, Radwanski R J, de Boer F R, Jacobs T H and Buschow K H J 1990 *J. Magn. Magn. Mater.* **86** 333
- [4] Shen B G, Kong L S and Cao L 1992 *Solid State Commun.* **83** 753
- [5] Li H S and Coey J M D 1991 *Handbook of Magnetic Materials* vol 6, ed K H J Buschow (Amsterdam: Elsevier) p 1
- [6] Shen B G, Wang F W, Kong L S and Cao L 1993 *J. Phys.: Condens. Matter* **5** L685
- [7] Wang Z and Dunlap R A 1993 *J. Phys.: Condens. Matter* **5** 2407
- [8] Gubbens P C M and van der Kraan A M 1990 *J. Less-Common Met.* **159** 173
- [9] Shen B G, Cheng Z H, Liang B, Guo H Q, Zhang J X, Gong H Y, Wang F W, Yan Q W and Zhan W S 1995 *Appl. Phys. Lett.* **67** 1621
- [10] Klesnar H, Hiebl K, Rogl P and Noël H 1989 *J. Less-Common Met.* **154** 217
- [11] Gao Y H, Tang N, Zhong X P, Wang J L, Li W Z, Qin W D, Yang F M, Zhang D M and de Boer F R 1994 *J. Magn. Magn. Mater.* **137** 275
- [12] Li H S, Mohanty R C, Raman A, Grenier C G and Ferrell R E 1997 *J. Magn. Magn. Mater.* **166** 365
- [13] Wang J L, Zhao R W, Tang N, Li W Z, Gao Y H, Yang F M and de Boer F R 1994 *J. Appl. Phys.* **76** 6470
- [14] Zhang Y D, Budnick J I, Ford J C and Hines W A 1991 *J. Magn. Magn. Mater.* **100** 13
- [15] Beuerle T and Fähnle M 1992 *J. Magn. Magn. Mater.* **110** L29
- [16] Shen N X, Zhang Y D, Budnick J I, Hines W A, Lyver R and Buschow K H J 1996 *Appl. Phys. Lett.* **69** 3194
- [17] Zhang Y D, Budnick J I, Yang D P, Fernando G W, Hines W A, Xiao T D and Manzur T 1995 *Phys. Rev. B* **51** 12091
- [18] Rao G N 1979 *Hyperfine Interact.* **7** 141
- [19] Capehart T W, Mishra R K and Pinkerton F E 1991 *Appl. Phys. Lett.* **58** 1395
- [20] Hu B P, Li H S, Sun H and Coey J M D 1991 *J. Phys.: Condens. Matter* **3** 3983
- [21] Shen B G, Cheng Z H, Liang B, Gong H Y, Wang F W, Tang H, Cao L, de Boer F R and Buschow K H J 1997 *J. Appl. Phys.* **81** 5173
- [22] Morariu M, Rogalski M S, Plugaru N, Valeanu M and Lazar D P 1994 *Solid State Commun.* **92** 889
- [23] Ge S H, Mao M X, Cheng Z H, Li C X, Sun J J, Li F S and Lin Q 1993 *Hyperfine Interact.* **78** 445
- [24] Strnat K 1986 *Ferromagnetic Materials* vol 4, ed E P Wohlfarth and K H J Buschow (Amsterdam: North-Holland) p 131
- [25] Hu Z, Yelon W B, Mishra S, Long G J, Pringle O A, Middleton D P, Buschow K H J and Grandjean F 1994 *J. Appl. Phys.* **76** 443
- [26] Coehoorn R 1989 *Phys. Rev. B* **39** 13072
- [27] Moze O, Caciuffo R, Gillon B, Calestani G, Kayzel F E and Franse J J M 1994 *Phys. Rev. B* **50** 9293
- [28] Freeman A J private communication